

EVOLUTION OF EXTRAGALACTIC RADIO SOURCES

THESIS

Submitted in partial fulfilment of the requirements
for the degree of

DOCTOR OF PHILOSOPHY

by

DILIP GOPAL BANHATTI



Department of Physics
INDIAN INSTITUTE OF TECHNOLOG
BOMBAY

NCRA LIBRARY



001035
520/525(043.2)

524.7-77

BAN

1984

THESIS APPROVAL SHEET

Thesis entitled "EVOLUTION OF EXTRAGALACTIC RADIO SOURCES" by DILIP GOPAL BANHATTI is approved for the degree of DOCTOR OF PHILOSOPHY.

Examiners

Supervisor (s)

Chairman

Date

SYNOPSIS

The evolution of extragalactic radio sources has two interconnected aspects. One is the origin and evolution of such an object, and the other is the change in the gross properties of populations of such sources at different epochs of the universe, assuming some (generally, a uniform relativistic) world model. This thesis considers both these aspects, the first one in more detail.

Most extragalactic radio sources have a double structure with two outer components and a galaxy or quasar (the parent object) roughly midway. If the process of generation of the two outer components in these double radio sources is intrinsically symmetric, the observed asymmetry among them can be attributed to projection effects. We have attempted to remove these projection effects in the brightness structure of some statistically well-defined samples of double radio sources and have arrived at two intrinsic parameters related to component production and evolution. We find that the average speed of advance of the hot spots, assuming intrinsic symmetry, must be about $0.15c$ if we are to explain the asymmetry in the positions of the two hot spots [1] and that the radio luminosity of the components must decrease as fast as the inverse cube of the intrinsic component-age to explain the asymmetry in the strengths of the components. If

part of the asymmetry is either intrinsic to the mechanism of component generation or is produced later due to an uneven distribution of the intergalactic medium on two sides of the parent object, the average speed and the rate of evolution of the component-luminosity would come down [2].

Various types of structure other than the simple double source also occur among extragalactic radio sources. In some sources, an S or Z symmetry exists around the parent object from about an arcsec to tens or hundreds of arcsec. Clearly, the central engine, which gives rise to the bifurcated double structure, sometimes precesses. A surprisingly wide variety of structures can arise from twin precessing relativistic jets of plasmons (evolving in some way) projected onto the plane of the sky. In this scheme, we have attempted to model the high redshift ($z = 1.595$) quasar 1857+566. This source has a 'warmspot' on one side and a jet with two sharp bends and no prominent hotspot on the other. We were able to model the jet but not the warmspot [3].

In studying the extended (tens to hundreds of arcsec) and the very compact (tens of milliarcsec) sources in detail, the sources of intermediate sizes (few arcsec) did not receive adequate attention and are only now being investigated in detail. We have observed an unbiased sample of 30 sources of sizes of few arcsec and stronger than 1 Jy at 91.8 cm selected from the Ooty lunar occultation survey. The technique of

interplanetary scintillation (IPS) was used for these observations carried out with the Ooty radio telescope. We find that about 45 percent of the total emission at 91.8 cm (326.5 MHz) arises from fine structure of overall size between 0.05 and 0.5 arcsec (median 0.18 arcsec). Comparison with earlier single-baseline VLBI (very long baseline interferometry) observations of these sources at 4.996 GHz indicate that the compact structure detected by IPS and VLBI is likely to be associated with the same physical features and that for about two-thirds of the sources which have steep spectra these features are hotspots or steep-spectrum kiloparsec cores while the remainder contain flat-spectrum compact components [4].

We have also observed with IPS at 91.8 cm another unbiased sample of 90 radio sources stronger than 0.75 Jy at that wavelength selected from list 9 of the Ooty lunar occultation survey. On an average, 30 percent of the emission from the sources comes from a region of angular size of about 0.3 arcsec. The sources cover a range in flux density from 0.75 to 4.5 Jy and the angular sizes go upto 500 arcsec. Dividing the 90 sources into three flux density ranges, we confirm the low flux density end of the correlation found between the fraction of scintillating flux density μ and the flux density S of extragalactic radio sources. The new point for the smallest S is in accordance with the levelling off of the μ - S relation toward small S found by previous

workers. The μ -S relation has bearing on the (cosmological) evolution of compact features in extragalactic radio sources with epoch. Another result from this IPS survey of 90 sources is that the scintillating size ψ is correlated with the largest angular size (LAS) of these sources. The median values of $\log \psi$ plotted against the median values of $\log \text{LAS}$ show a roughly linear relation with a slope much less than 1. The median $\log \psi$ and $\log \text{LAS}$ values for the sample of 30 few-arcsec sources are in accord with this relation. If the scintillating structure is interpreted as hotspots in double radio sources, this small slope has implications for the collimation of extragalactic jets. 81.5 MHz IPS data on the powerful edge-brightened double sources from the strong 3CR sample indicate a similar correlation between $\log \psi$ and $\log \text{LAS}$ [5]. However, 4.87 GHz VLA data on the most compact and/or intense hotspots from a sample of sources show that the hotspot size ψ_{HS} and the distance of the hotspot from the core θ are related. A plot of $\log \psi_{\text{HS}}$ vs $\log \theta$ shows a slope close to 1. The small slopes obtained from the IPS data are probably due to projection effects and because the IPS technique averages over all the compact structure in the telescope beam [6].

The luminosity function of extragalactic radio sources gives the space density of the sources as a function of luminosity and redshift (which determines the epoch) for a given world model. It has been found that for uniform relativistic

world models, the luminosity function depends strongly on epoch, the high luminosity sources being about two and a half orders of magnitude more numerous at a redshift of about 2 than at present. This cosmological evolution is stronger for the extended steep-spectrum source population than for the compact flat-spectrum sources. However, some world models do not require any evolution. We have performed the luminosity-volume test within the world model given by Hoyle-Narlikar conformal gravity and find that no evolution is required for both steep- and flat-spectrum sources [7].

References

- [1] D.G. Banhatti, Expansion speeds in extended extragalactic radio sources from angular structure, A.&A., 84 (1980), 112-114.
- [2] G. Swarup and D.G. Banhatti, Evolution of extended extragalactic double radio sources, M.N.R.A.S., 194 (1981), 1025-1032.
- [3] D.J. Saikia, P. Shastri, T.J. Cornwell and D.G. Banhatti, An interesting radio jet in the high-redshift quasar 1857+566, M.N.R.A.S., 203 (1983), 53P-57P.
- [4] D.G. Banhatti, S. Ananthakrishnan and A. Pramesh Rao, M.N.R.A.S., 205 (1983), 585-591.
- [5] D.G. Banhatti, The ψ_{IPS} -LAS relation for extragalactic radio sources, M.N.R.A.S. in press (for 15 Nov. '84 issue).

- [6] D.G. Banhatti, Collimation of extragalactic jets: evidence from hotspots, M.N.R.A.S., 208 (1984), 7P-10P.
- [7] V.K. Kulkarni and D.G. Banhatti, The V/V_m test in Hoyle-Narlikar conformal gravity, Ap. J. 274 (1983), 469-473.

CONTENTS

Synopsis	i
List of tables	ix
List of figures	x
1.0	Introduction: extragalactic radio sources: symmetric double structure...	1- 1
1.1	Symmetric double structure...	1- 2
1.2	Radio spectrum	1- 5
1.3	Hotspots	1-10
1.4	Outline of the thesis	1-11
2.0	The asymmetry in extended extragalactic double radio sources I	2- 1
2.1	The relativistic expansion model	2- 5
2.2	The fractional arm and difference x	2- 6
2.2.1	Application to a strong source sample	2- 9
2.2.2	Error analysis in brief	2-16
2.3	Predicted linear size distribution	2-17
3.0	The asymmetry in extended extragalactic double radio sources II	3- 1
3.1	The flux ratios and arm ratios	3- 8
3.2	The positional offset between the optical identification and radio centroid	3-12
3.3	Interpretation of the r, s - distribution in the relativistic expansion model	3-15
3.4	Inhomogeneities in the IGM as cause of the asymmetry	3-23
4.0	The relativistic twin precessing beams model	4- 1
4.1	The model	4- 1
4.2	Application to the high-redshift quasar 1857+566	4- 7

5.0	IPS observations of Ooty occultation radio sources	5- 1
5.1	IPS theory in brief	5- 2
5.2	IPS observation and reduction procedure	5- 6
5.3	30 sources of sizes of few arcsec: observations	5-10
5.3.1	Interpretation	5-17
5.4	An unbiased sample of 90 Ooty occultation radio sources: observations	5-28
5.4.1	The statistics of ψ and μ	5.35
5.4.2	The ψ_{IPS} - LAS relation for extragalactic radio sources	5-44
5.4.3	The difference between the Ooty and 3CR samples	5-47
5.4.4	The ψ_{HS} - θ relation from VLA observations of hotspots	5-56
5.4.5	Connection between the ψ_{HS} - θ and ψ_{IPS} - LAS relations	5-63
6.0	Cosmological evolution of extragalactic radio sources	6- 1
6.1	The V/V_m test in HN gravity	6- 4
6.2	The V/V_m test for nonmonotonic $S_V(z)$	6- 9
	Conclusions	C - 1
	References	xiii
	Acknowledgements	xviii

List of tables

<u>No.</u>	<u>Title</u>	<u>Page No.</u>
2.1	The sample of extended double radio sources used for deriving the distribution of separation speeds of the hotspots	2-10
2.2	Rough fits for the observed linear size distributions of Figs. 2.7a-d. Curves for various model parameters are shown in Figs. 2.6a-d.	2-31
3.1	Data for the Ooty double radio sources	
	(a) The optically identified sources	3- 3
	(b) The unidentified sources	3- 4
3.2	Data for the 3CR double radio sources	3-11
5.1	Observation log for the 30 sources	5-12
5.2	Data for the 30 sources	5-18
5.3	%VLBI detections for different ranges of the predicted 326.5 MHz correlated flux density	5-24
5.4	% VLBI detections and % optical identifications for the two spectral classes	5-26
5.5	Observation log for the 90 sources	5-29
5.6	Data for the 90 Ooty occultation sources	5-36
5.7	Properties of the 3 LAS classes of the 90 Ooty occultation radio sources	5-41
5.8	The hotspots used (for the $\Psi_{\text{HS}}-\theta$ relation)	5-60
6.1	V/V_m for Wills and Lynds samples	6- 6

List of figures

<u>No.</u>	<u>Title</u>	<u>Page No.</u>
1.1	A 5 GHz map of 1957+405 (= Cyg A = 3C 405) from Hargrave & Ryle (1974). See also Perley et al. (1984) for a recent VLA map	1- 3
1.2	326.5 MHz lunar occultation scans of 0106+130 (= 3C 33). The observations were done at Ooty and reported by Gopal-Krishna et al. (1976) and Gopal-Krishna and Swarup (1977)	1- 4
1.3	Radio spectra of components of 1957+405 and the total spectrum	1- 6
1.4	Radio spectra of components of 0106+130 and the total spectrum	1- 7
2.1	Geometry and terminology of the relativistic expansion model	2- 4
2.2	Limits of integral in deriving equation 2.6	2- 7
2.3	Observed distributions and fits for the fractional arm difference x for samples of doubles listed in Table 2.1	2-12
2.4	Distribution of the hotspot separation speeds v for samples of doubles listed in Table 2.1	2-14
2.5	$1/\ell_o$ vs v or T_{LMyr} vs v for $\ell_{oMpc} = 1.0$	2-21
2.6	Model distributions of projected and actual linear sizes for $v=0.1, 0.3, 0.5$ & 0.7 and...	
(a)	... $\ell_{oMpc} = 0.8$	2-23
(b)	... $\ell_{oMpc} = 0.9$	2-24
(c)	... $\ell_{oMpc} = 1.0$	2-25
(d)	... $\ell_{oMpc} = 1.2$	2-26
2.7	Observed distributions of projected linear sizes for four samples:	
(a)	126+4 FR II 3CR sources	2-27

<u>No.</u>	<u>Title</u>	<u>Page No.</u>
2.7(b)	Ekers & Miley's (1977) 85+2 3CR sources	2-28
(c)	Longair & Riley's (1979) 65+1 3CR sources	2-29
(d)	72 well-separated 3CR doubles used in section 2.2	2-30
3.1	The observed distribution of flux ratios f for the Ooty (326.5 MHz) doubles and the 10 times brighter 3CR (5 GHz) doubles	3- 6
3.2	The joint distribution of arm ratios r and flux ratios s (on a log-log scale) for the faint Ooty (326.5 MHz) doubles and the 10 times brighter 3CR (5 GHz) doubles	3- 9
3.3	Observed linear size distributions of 3CR doubles divided into two classes: those with fainter component appreciably closer than the brighter, and the rest	3-14
3.4	Restrictions on t_0 and y from velocity cut-off	3-16
3.5	Observed distributions of arm ratios r for the faint Ooty and bright 3CR doubles and model fits to the 3CR data for $v_0 = 0.4c$ and $v_0 = 0.16c$	3-18
3.6	Observed distributions of flux ratios s on a log-scale for the faint Ooty and the bright 3CR doubles and model fits to the 3CR data for $v_0 = 0.6c$, $\delta = 3$ and $v_0 = 0.16c$, $\delta = 1$	3-19
3.7	Joint distribution of $\log r$ and $\log s$ and model fits	3-20
4.1	Geometry of the relativistic precessing beams model	4- 3
4.2	(a) $\lambda 6$ cm map of 1857+566 from Saikia et al. (1983), and (b) contour plot of the model fit, with levels chosen to match those of the observed map	4- 8
5.1	Thin screen model for scattering of radio waves by the interplanetary medium	5- 3

<u>No.</u>	<u>Title</u>	<u>Page No.</u>
5.2	Observed distributions of the compactness parameter μ and the (mean) angular size of compact features ψ for the 30 few arcsec sources	5-16
5.3	S_{c327} vs S_{c4996} on log-log scale	5-22
5.4	Observed distributions of the compactness parameter μ and the (mean) angular size of compact features ψ for the 90 Ooty sources divided into 3 LAS classes	5-39
5.5	ψ vs μ scatter diagram for the 90 Ooty IPS sources	5-40
5.6	μ vs α scatter diagram for the 90 Ooty IPS sources	5-42
5.7	ψ vs α scatter diagram for the 90 Ooty IPS sources	5-43
5.8	$\psi_{326.5}$ - LAS relation (median values) on log-log scale	5-45
5.9	$\psi_{81.5}$ - LAS relation (median values) on log-log scale	5-46
5.10	Observed distribution of spectral indices α_{2700}^{327} for the unbiased sample of 90 faint Ooty sources	5-49
5.11	Scatter diagram for the 128 identified FR II 3CR ₁ sources: $\mu_{81.5} - \log P_{178}$	5-52
5.12	$\log P_{178} - \log \text{LAS}$	5-53
5.13	$\psi_{81.5} - \log P_{178}$	5-54
5.14	$f - \ell$ diagram for the 31 hotspots of Swarup et al. (1984)	5-57
5.15	$\psi_{\text{HS}} - \theta$ relation (on log-log scale) for the 14 brightest and/or most compact hotspots from Swarup et al. (1984)	5-59
6.1	$S_{\nu}(z)$ relation in Hoyle-Narlikar conformal gravity	6- 5
6.2	$S_{\nu}(z)$ relation with one minimum	6-10

CHAPTER ONE

INTRODUCTION: EXTRAGALACTIC RADIO SOURCES:

SYMMETRIC DOUBLE STRUCTURE

1.0 After Karl Jansky's discovery in 1933 that the centre of our Galaxy emitted radio noise at $\lambda 15\text{m}$, which in addition to man-made radio interference and thunderstorms, caused unwanted radio noise in communication receivers, Grote Reber in 1937 discovered that the sky emitted a diffuse continuum at $\lambda 1.9\text{m}$ in all directions, predominantly in the Galactic plane. The sun was discovered to be a radio emitter at $\lambda \lambda 4$ to 8m during J S Hey's study in 1942 of the jamming of army radar sets. These findings were the beginning of radio astronomy. As the sensitivity of the telescopes improved, thousands of discrete radio sources were discovered. These sources are marginally concentrated toward the Galactic plane. Among those Galactic sources are gaseous nebulae like the Orion, supernova remnants like Taurus A (Crab nebula) and Cassiopeia A and clouds of ionized hydrogen (H II regions). Those away from the Galactic plane are found to be distributed uniformly on the sky, similar to the 2.7 K microwave radiation background. Most of these discrete sources (Galactic latitude $|b^{\text{II}}| > 10^\circ$ or so) were recognized to be extragalactic. Measurements on photographs taken in the optical band showed that in many cases galaxies and bright blue stellar objects (quasars) are coincident with or very close to the centroid of radio emission. More

recently, many of these galaxies and quasars have been found to emit also in the X-ray, ultraviolet and/or infrared regions of the electromagnetic spectrum (Ku, Helfand & Lucy 1980, Gondhalekar 1981, Houck et al. 1984, Soifer et al. 1984, Young et al. 1984, Miley et al. 1984, Neugebauer et al. 1984, Gear et al. 1984 & references therein).

1.1 SYMMETRIC DOUBLE STRUCTURE About 30 years ago, Jennison & Das Gupta (1953) made the fundamental and exciting discovery that Cygnus A, the strongest observed extragalactic radio source, consists of two components which symmetrically straddle the associated optical galaxy and exceed it in their size by a factor of about two. They also found that the distance between the outer ends of the components exceeds the size of the optical galaxy by a factor of about five. As was revealed with finer and finer resolution aperture synthesis observations over the ensuing years, this double structure was by far the hallmark of the majority of extragalactic radio sources found in surveys carried out at low frequencies (≤ 1 GHz). Most of these extended radio sources have physical sizes (projected onto the sky-plane) of 225-450 kpc (with $H_0 = 50$ km/s/Mpc) with a median size of about 250 kpc, though there are also sources as small as the size of the associated optical galaxy (typically 30 kpc) and the largest go upto 6 Mpc (see Miley 1980). However, sources selected at higher frequencies (≥ 1 GHz) are dominated by another class of radio sources, with sizes

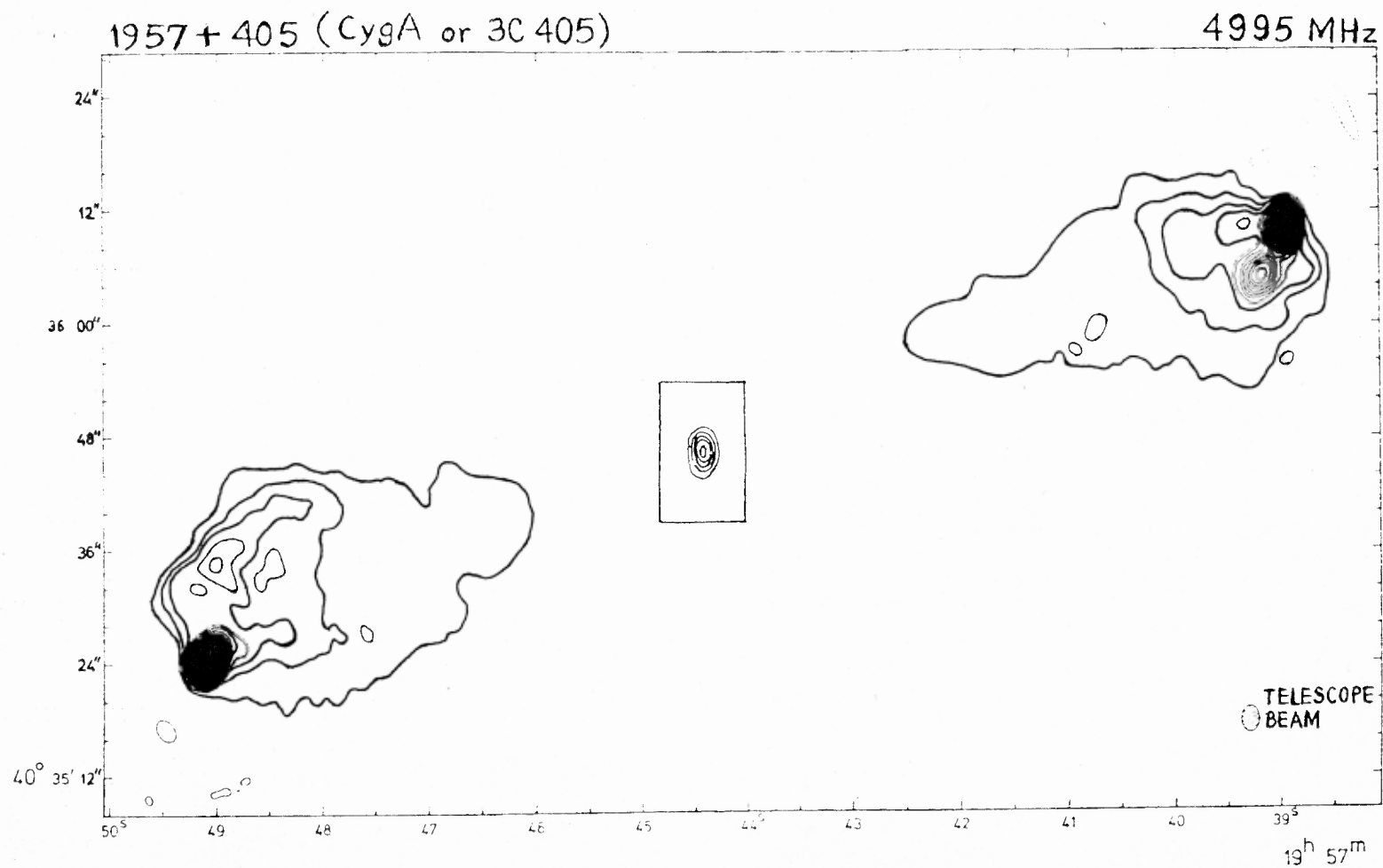


Fig 1.1 A 5 GHz map of 1957+405 (\equiv CygA \equiv 3C 405) from Hargrave & Ryle (1974). See also Perley et al. (1984) for a recent VLA map.

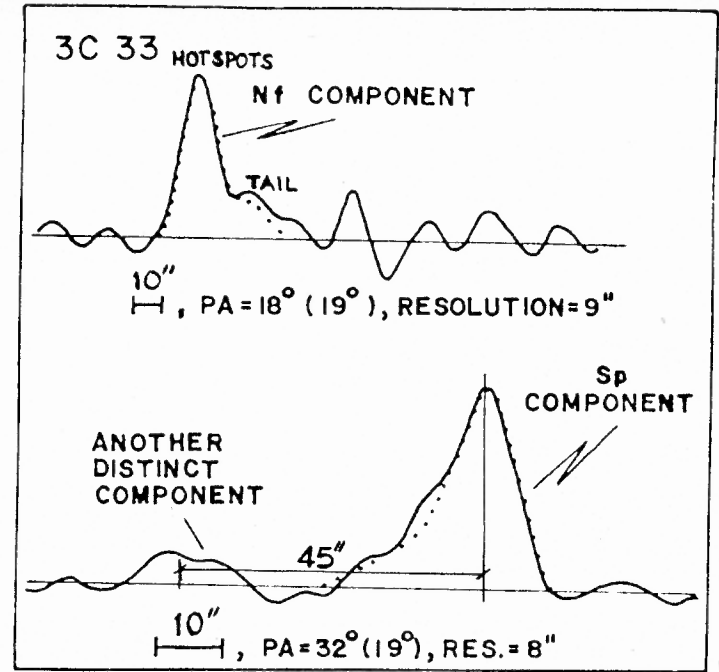
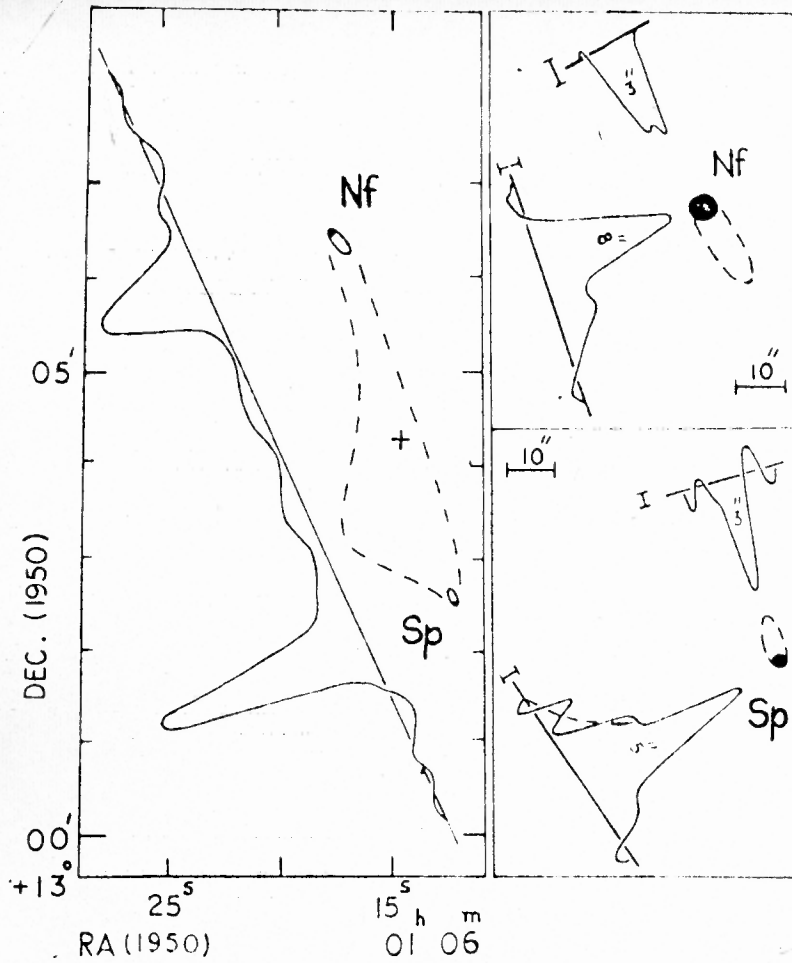


Fig 1.2 326.5 MHz lunar occultation scans of 0106+130 (\equiv 3C33). The observations were done at Ooty and reported by Gopal-Krishna, Joshi & Ananthakrishnan (1976 ApLett 17 11) and Gopal-Krishna & Swarup (1977 MN 178 265).

varying from about a parsec to tens of kpc, being much smaller than the extended radio sources typified by Cyg A. Even other kinds of source structure (like head-tail sources) among the extended radio sources are sought to be explained as a variation of the basic double structure. (See Miley 1980). Some of the details revealed by the fine resolution and high sensitivity observations include two hotspots at the outer edges of the two radio components, fainter extensions (radio lobes) from the two outer peaks trailing away toward the central radio peak found coincident with the central galaxy or quasar, and often a jet or jets pointing from the middle peak to one or both of the hotspots. This bifurcated symmetric structure is exemplified in Fig. 1.1 by a 5 GHz map of the radio source Cyg A, and in Fig. 1.2 by 326.5 MHz lunar occultation scans of 3C33. We notice that the hotspots can be multiple (see section 1.3).

1.2 RADIO SPECTRUM A very important property of extragalactic radio sources apart from their structure is their radio spectrum. For a vast majority of sources, the flux density S is a power law over a wide range of frequencies ν . The spectral index α over this frequency range is defined by $S \propto \nu^{-\alpha}$. A two-point spectral index is defined by

$$\alpha = - \frac{\log (S_1/S_2)}{\log (\nu_1/\nu_2)}$$

The very compact sources generally have $\alpha < 0.5$ and the extended

Spectra of components of
1957+405 (Cyg A, 3C 405)

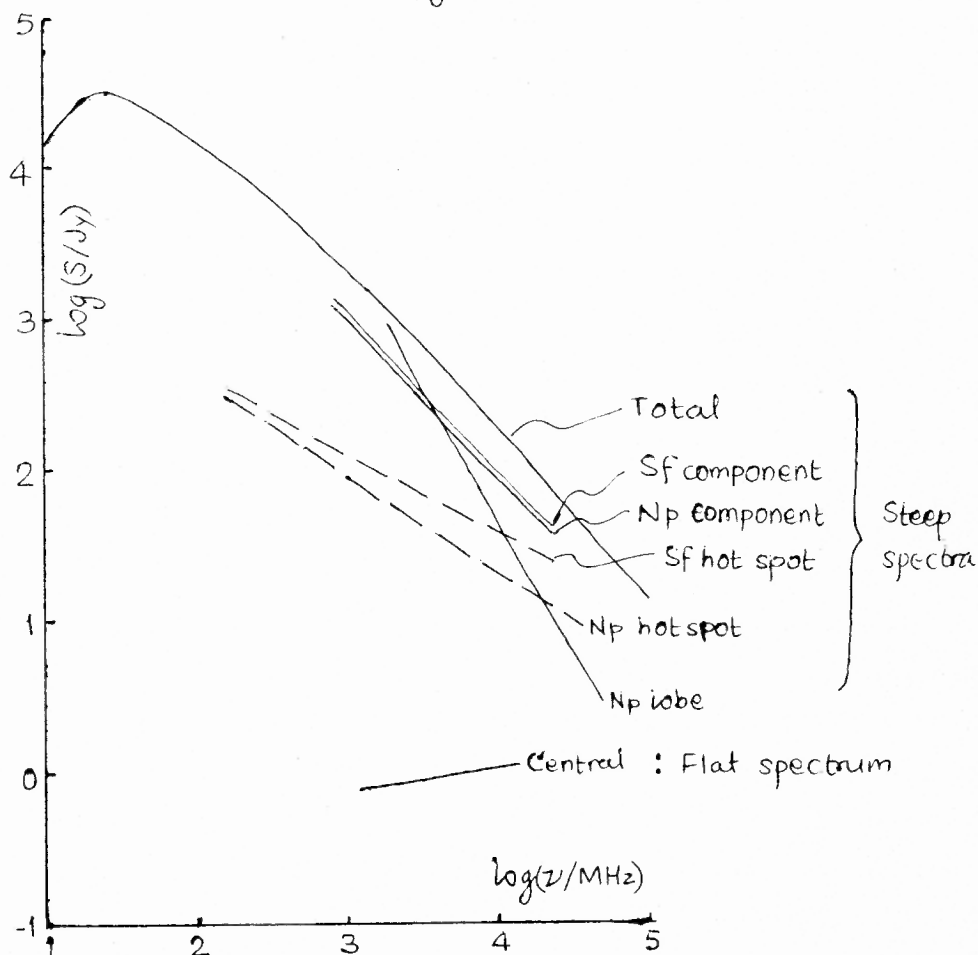


Fig. 1.3 Radio spectra of components of 1957+405 (\equiv Cyg A \equiv 3C 405) and the total spectrum. Data from Rowson (1963), Mitton & Ryle (1969), Hargrave & Ryle (1974, 1976), Baker et al. (1975), Bentley et al. (1975).

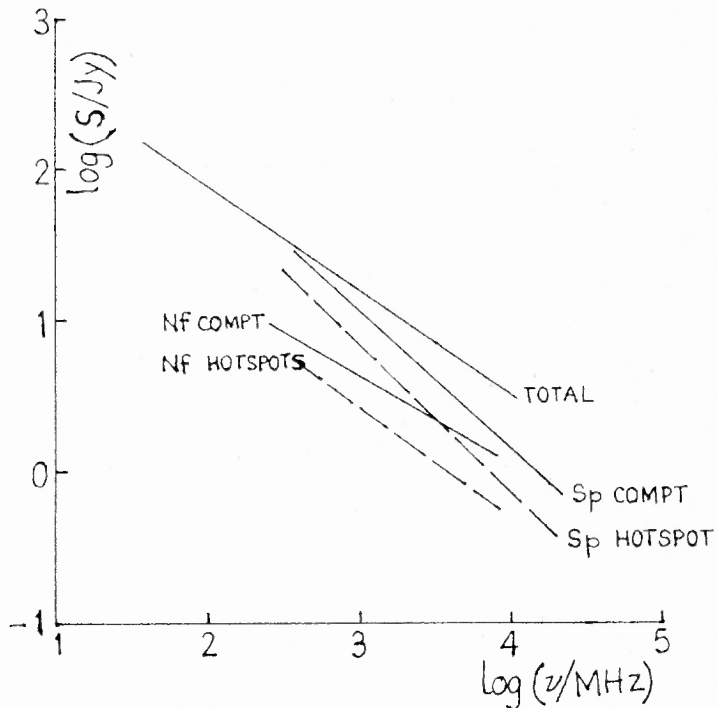


Fig. 1.4 Radio spectra of components of 0106+130 (\equiv 3C 33) and the total spectrum. Data from Kellerman, Pauliny-Toth & Williams (1969 ApJ 157 1), Macdonald, Kenderdine & Neville (1968), Mitton (1970 ApLett 5 207), Hargrave & McEllin (1975 MN 173 37), Gopal-Krishna et al. (1976 ApLett 17 11), Laing (1981) and Dreher (1981)

sources have $\alpha \geq 0.5$. Hence the nomenclature compact flat-spectrum sources ($\alpha \leq 0.5$) and extended steep-spectrum sources ($\alpha > 0.5$) (Figs. 1.3 and 1.4). Scheuer & Readhead (1979) have suggested that compact sources could intrinsically be the same as extended sources, differing only in their small orientation to the line of sight. This is often referred to as the relativistic beaming model or Doppler favouritism and has been worked out in detail by Blandford & Koenigl (1979). Based on this idea, a unified scheme to account for various properties of compact and extended extragalactic radio sources has been worked out (Orr & Browne 1982). In this scheme, the sources close to the plane of the sky have the largest angular sizes and have a predominantly steep spectrum whereas the sources oriented close to the line of sight are compact and have a flat spectrum. The central component, when detected, generally falls into the compact flat-spectrum class. The spectral index of hotspots is generally between 0.6 and 0.8 while that of the lobes is often 0.9 (Figs. 1.3 and 1.4). The overall spectral index of the extended steep-spectrum sources is about 0.8. Recent observations have shown that there is also a third class among extragalactic radio sources: the compact steep-spectrum class (Kapahi 1981, Peacock & Wall 1982), more prominent in high frequency (> 1 GHz) surveys. Since the first two were recognized early, attention was focused on them, and the compact steep-spectrum sources are only now being studied in as much detail (see section 5.3). The nature of these sources

is not yet clear.

The simplest form of the radio spectrum of a component consists of a power law down to some frequency at which the flux density drops abruptly (the low frequency cut-off) (see Figs. 1.3 and 1.4). These two features of the spectrum are quite adequately explained by supposing that the radiation comes from relativistic charged particles with a power law energy spectrum moving in a magnetic field. Evidence for the presence and orientation of the magnetic field comes from polarization observations. This is called synchrotron radiation (Ginzburg & Syrovatskii 1965, Scheuer 1967, Moffet 1975). Quite many complex spectra with several power laws in different frequency ranges and several peaks in the spectrum can be explained as a superposition of simple power law spectra with low frequency cut-offs at different frequencies. Physically, this means that the radiation comes from several populations of relativistic charged particles occupying regions of space of various sizes. The power law energy spectrum of the relativistic charged particles finds a natural explanation in the simple acceleration mechanism of particles repeatedly crossing a shock front (Bell 1978, Michel 1981, Peacock 1981, Webb, Drury & Biermann 1984, Webb & McKenzie 1984). (See also Alfvén & Herlofson 1950 who anticipated many of the present ideas concerning the radiation mechanism in radio sources.)

1.3 HOTSPOTS Until about 1975 the outer edges in powerful double radio sources, called hotspots, were merely seen as the brightest features, barely resolved with the resolution then available (few arcsec to tens of arcsec for Ooty lunar occultation, WSRT and the Cambridge One Mile and 5-km telescopes) (Joshi & Singal 1980 and references therein, Katgert & Spinrad 1974, Macdonald, Kenderdine & Neville 1968, Mackay 1969, Branson et al. 1972 and references therein, Jenkins, Pooley & Riley 1977 and references therein, Laing 1981). As the resolution of aperture synthesis observations became finer (sub-arcsec with the VLA and MERLIN), hotspots started showing internal fine structure (Kerr et al. 1981, Dreher 1981, Barthel & Lonsdale 1983, Lonsdale & Barthel 1984, Perley, Dreher & Cowan 1984), smaller than about few kpc ($H_0 = 50 \text{ km/s/Mpc}$). Observations of hotspots with VLBI showed that there is structure on still smaller scales of few hundred pc (Kapahi & Schilizzi 1979, Barthel 1983). Looking at the observations of radio sources on all these scales showed the relationship between the central radio component (site of the parent, central engine), the jets (beams carrying energy from the central engine to the outer components) and the hotspots (places where the beam decelerates and thereby dissipates its energy). The structures and shapes of hotspots and their relation to the jet direction vary from source to source (Laing 1981, Barthel 1984, Swarup, Sinha & Hildrup 1984). The spectrum of hotspots is the flattest (α least - see section 1.2 and Figs. 1.3 and

1.4 above) among all the features of the outer components, consistent with the beam model, since emission from the youngest relativistic particles leads to the flattest spectrum according to synchrotron theory (Moffet 1975). The hotspot size increases roughly proportionally to the distance from the central component (or galaxy or quasar) (see section 5.4.4), the mean ratio of distance to size being about 50. In the beam model, hotspots are formed at the end of a beam of relativistic particles and magnetic field as it slows down due to the intergalactic medium. They thus move through the medium in dynamic equilibrium, the ram pressure of the jet/beam balancing the pressure due to the medium at the hotspot.

1.4 OUTLINE OF THE THESIS The evolution of extragalactic radio sources has two interconnected aspects. One is the origin and evolution of such an object, and the other is the change in gross properties of populations of such sources with the cosmic epoch, assuming some (generally a uniform relativistic) world model. This thesis considers both these aspects, the first one in much more detail. In Chapters 2 and 3, we explore the implications of the observed asymmetry in the angular structure and the brightness structure of extended extragalactic double radio sources. We assume that the process of their production is intrinsically symmetric, the observed asymmetry in the angular structure arising due to the orientation of the double source axis away from the sky plane. After presenting

a model to interpret the angular and brightness asymmetry of double radio sources (section 2.1), we explore this argument in detail to derive the distribution of hotspot speeds (sections 2.2 and 2.2.1) and briefly discuss the sources of error (section# 2.2.2). For a constant speed model, a definite linear size distribution is implied. This is derived and discussed in section 2.3.

In Chapter 3, we first present the observed distributions of flux density ratios s and f (which characterize the brightness asymmetry) and the arm ratios r (to quantify the angular asymmetry) (sections 3 and 3.1) for two well-defined samples of bright classical doubles. The flux ratio f for a source is defined to be greater than one, the flux density of the brighter component to that of the fainter one. The arm ratio r is defined to be less than one, the shorter arm to the longer one, and s is defined in conjunction with r - flux density of the nearer component to that of the farther one. The parameters r and s together approximately define the relative displacement of the radio centroid from the optically identified galaxy or quasar. We find that the relative displacement for fainter (that is, deeper) low frequency samples agrees with that for the bright classical doubles (section 3.2). This is consistent with the faint low frequency samples predominantly containing the same type of sources.

In the model of section 2.1, the brightness asymmetry arises because the two components are observed at different stages of their evolution, and can thereby be used, together with the angular asymmetry and the implied hotspot speeds, to infer the extent of evolution required. There is also a contribution to the asymmetry due to the Doppler effect (section 3.3). Even without an underlying intrinsically symmetric model, the angular and brightness asymmetries provide valuable observational input which must be explained by theory. We summarize literature on description of these asymmetries (end of section 3.3). An alternative explanation for the asymmetry in double radio sources could be inhomogeneities in the surrounding intergalactic medium. At the end of Chapter 3 (section 3.4) we briefly estimate the clumpiness required in the medium to explain the angular and brightness asymmetry.

With aperture synthesis observations of subarcsec resolution, it has become possible to adequately map the narrow features (jets) in the extended steep-spectrum double radio sources. An inversion symmetry ('S' shape, e.g.) has been found in many sources and leads naturally to the introduction of precession of the central engine in the simple version of the beam model. If the beam speed is highly relativistic, even highly asymmetric structures can be modelled. We have attempted to model the highly asymmetric high-redshift quasar

1857+566 within the framework of twin precessing relativistic beams (Chapter 4).

A majority of extragalactic radio sources selected at low frequencies have a steep spectrum and most of these have a weak or undetectable central component of flat spectrum, but generally the central component is too weak to be detected at metre-wavelengths (see section 1.2 and Figs. 1.1-1.4). Any fine structure at metre-wavelengths thus refers to the steep-spectrum hotspots. In Chapter 5 we present observations of two samples of radio sources selected from the Ooty lunar occultation survey at λ 91.8 cm. These observations were made with the Ooty Radio Telescope using the technique of interplanetary scintillations (IPS) (section 5.1). IPS gives two gross measures of the fine structure in the telescope beam: the overall size of the scintillating structure, ψ , and the fraction, μ , of flux density within that size (section 5.2). As mentioned at the end of section 1.2, the compact steep-spectrum sources have not been adequately studied. The sizes of these sources are intermediate between the very compact (tens of milliarcsec) flat-spectrum sources and the extended (tens to hundreds of arcsec) steep-spectrum ones. We have observed an unbiased sample of 30 weak radio sources with sizes of a few arcsec using the IPS technique (section 5.3) and interpret the observations in conjunction with earlier high-frequency single-baseline measurements using the technique

of very long baseline interferometry (VLBI) (section 5.3.1). To examine the fine structure in sources selected at low frequencies over a large range of angular sizes and flux densities, we have made IPS observations of an unbiased sample of 90 weak radio sources selected from the ninth list of the lunar occultation survey (Joshi & Singal 1980) (section 5.4). On an average, the scintillating fine structure contains 30% of the flux density within about 0.3 arcsec. The flux density range of the sample spans a factor of about 5:1 and we get three points in the faint end of the scintillating fraction - flux density relationship, confirming earlier results that this relation saturates at the lower end (section 5.4.1). We explore the implications of the IPS observations of the 90 faint radio sources in conjunction with IPS observations of other brighter samples (sections 5.4.1-5.4.3). In particular, we find that the scintillating size is weakly correlated with the total angular size for both the faint Ooty and bright 3CR samples, using the IPS observations of the 3CR sample from the literature (section 5.4.2). The slopes of the linear relations between the median values on a log-log plot are 0.2 and 0.4 respectively for the two samples and there is also a break between the two lines. We examine possible reasons for the difference in slopes as well as the break and show that the main reasons are different mean angular sizes and different methods of determining the scintillating size (for the break) and the larger redshift range for the

brighter 3CR sample compared to the fainter Ooty sample (for the different slopes) (section 5.4.3). After presenting a rough proportionality between the hotspot size and the distance from core to hotspot for high resolution observations of a sample of double radio sources of the largest angular sizes (section 5.4.4), we point out the connection between this relation and the scintillating size - total angular size correlation and the bearing of these results on the collimation of extragalactic jets (section 5.4.5).

We now go on to the part of this thesis (Chapter 6) dealing with cosmological evolution of extragalactic radio sources. By this is meant the change in the gross properties of populations of these sources with cosmic epoch. A world model which determines the underlying space-time geometry must be assumed in studies of cosmological evolution. The standard choice is a uniform relativistic world model, and leads to the requirement of strong evolution in the space density and luminosity of radio source populations with cosmic epoch to explain the observed properties of populations of radio sources. However, some unconventional world models may not require any evolution to reconcile theory with observations. We consider one such model, that given by Hoyle-Narlikar conformal gravity, and show that in this world model the luminosity-volume (V/V_m) test is consistent with no evolution for both steep- and flat-spectrum sources (section

6.1). We also show that the V/V_m test can be applied for an arbitrary nonmonotonic $S(z)$ (flux density S vs z , the redshift - for a fixed luminosity) and indicate how it can be done (section 6.2).